

Piotr S. Szczepaniak
Paulo J. G. Lisboa
Janusz Kacprzyk (Eds.)

Fuzzy Systems in Medicine

With 299 Figures
and 64 Tables

Physica-Verlag
A Springer-Verlag Company

Piotr S. Szczepaniak, PhD, DSc
Associate Professor
Institute of Computer Science
Technical University of Łódź
ul. Sterlinga 16/18
90-217 Łódź
Poland
office@ics.p.lodz.pl

Prof. Paulo J. G. Lisboa
School of Computing and Mathematical Sciences
Liverpool John Moores University
Liverpool L3 3AF
United Kingdom
p.j.lisboa@livjm.ac.uk

Prof. Janusz Kacprzyk
Systems Research Institute
Polish Academy of Sciences
ul. Newelska 6
01-447 Warsaw
Poland
kacprzyk@ibspan.waw.pl

ISBN 3-7908-1263-3 Physica-Verlag Heidelberg New York

Cataloging-in-Publication Data applied for
Die Deutsche Bibliothek – CIP-Einheitsaufnahme
Fuzzy systems in medicine: with 64 tables / Piotr S. Szczepaniak; Paulo J. G. Lisboa; Janusz Kacprzyk (eds.) – Heidelberg; New York: Physica-Verl., 2000
(Studies in fuzziness and soft computing; Vol. 41)
ISBN 3-7908-1263-3

This work is subject to copyright. All rights are reserved, whether the whole or part of the material is concerned, specifically the rights of translation, reprinting, reuse of illustrations, recitation, broadcasting, reproduction on microfilm or in any other way, and storage in data banks. Duplication of this publication or parts thereof is permitted only under the provisions of the German Copyright Law of September 9, 1965, in its current version, and permission for use must always be obtained from Physica-Verlag. Violations are liable for prosecution under the German Copyright Law.

© Physica-Verlag Heidelberg 2000
Printed in Germany

The use of general descriptive names, registered names, trademarks, etc. in this publication does not imply, even in the absence of a specific statement, that such names are exempt from the relevant protective laws and regulations and therefore free for general use.

Hardcover-Design: Erich Kirchner, Heidelberg

SPIN 10748155

88/2202-5 4 3 2 1 0 – Printed on acid-free paper

Part 2 CASE STUDIES

SIGNAL PROCESSING

- Entropy and Energy Measures of Fuzziness in ECG Signal Processing 227
E. Czogala, J. Leski
- Fuzzy Logic System for ECG Interpretation 246
A. Grauel
- EEG Analysis for Assessment of Depth of Anaesthesia 261
J. Petersen, G. Stockmanns, W. Nahm

IMAGE PROCESSING AND INTERPRETATION

- Fuzzy Sets in Medical Image Processing 281
G. Berks, D.G.v. Keyserlingk
- Enhancement of Megavoltage Images in Radiation Therapy
Using Fuzzy and Neural Image Processing Techniques 316
H.R. Tizhoosh, G. Krell, B. Michaelis
- Fuzzy Clustering Methods for the Segmentation of Multimodal
Medical Images 335
F. Masulli, A. Schenone, A.M. Massone
- Fuzzy Clustering for Parametric Map Construction in Myocardial
Perfusion Magnetic Resonance Images 351
F. Behloul, A.-O. Boudraa, M. Janier, P. Croisille
- Neuro-Fuzzy Models of Radiographic Image Classification 361
P.R. Innocent, R.I. John, M. Barnes
- Segmentation of Medical Images Using Fuzzy Technique 394
F. Waidelich, H. Eichfeld, R. Graumann
- Fuzzy Quantification of Artery Lesions in Renal Arteriographies 410
M.-C. Jaulent, V. Bombardier, I. Cherrak, O. Perez-Oramas
- Fusion of Numerical and Structural Image Information
in Medical Imaging in the Framework of Fuzzy Sets 429
I. Bloch

CONTROL, DIAGNOSIS AND THERAPY

- Fuzzy Reasoning in Pacemaker Control 451
A. Bardossy, A. Blinowska

- Closed-Loop Control of Anaesthesia Using Fuzzy Logic 467
D.A. Linkens, M.F. Abbod, J.K. Backory, J.S. Shieh

- Self-Learning Fuzzy Logic Control of Anaesthetic
Intravenous Infusions 484
D.G. Mason, N.D. Edwards

- Fuzzy Inference Neural Networks and Their Applications to Medical
Diagnosis 503
D. Rutkowska, A. Starczewski

- Neuro-Fuzzy Modelling of Heart Rate Signals and Application to
Diagnostics 519
J.A. Swope, N.K. Kasabov, M.J.A. Williams

- Fuzzy Diagnosis by Score-Based Tests – Implementation Issues 543
S. Zahan

- A Comparison of Fuzzy Decision Models Supporting the
Optimal Therapy 561
E. Rakus-Andersson, T. Gerstenkorn

- A Neuro-Fuzzy System for Emulation of Human Grasp Movements 573
K. Cerbioni, C. Colosimo, A. Starita, P. Dario

KNOWLEDGE BASED SYSTEMS

- Fuzzy and Crisp Logical Rule Extraction Methods in Application
to Medical Data 593
W. Duch, R. Adamczak, K. Grąbczewski, G. Żal, Y. Hayashi

- Extending Description Logics to Vague Knowledge in Medicine 617
R. Molitor, C.B. Tresp

- Representation and Acquisition of Knowledge for a Fuzzy Medical
Consultation System 636
T.E. Rothenfluh, K. Bögl, K.-P. Adlassnig

- The Development of a Fuzzy Expert System for the Analysis of Umbilical
Cord Blood 652
J.M. Garibaldi, E.C. Ifeachor

- Fuzzy Expert System for Exercise Therapy in Diabetics 669
J. Novotný, F. Babinec

- Subject Index 693

20. Tizhoosh, H.R., Haußecker, H. (1998): Fuzzy Image Processing: An Overview. Will be published in: Jähne, B., Haußecker, H., Geißler, P. (Eds.), Handbook on Computer Vision and Applications, *Academic Press*, Boston, 1998.
21. Zadeh, L. A. (1965): Fuzzy sets. *Information and Control* 8, 338–353.

Fuzzy Clustering Methods for the Segmentation of Multimodal Medical Images

F. Masulli^{1,2}, A. Schenone³ and A.M. Massone¹

¹ Istituto Nazionale per la Fisica della Materia, Via Dodecaneso 33, 16146 Genova, ITALY

² Dipartimento di Informatica e Scienze dell'Informazione, Università di Genova, Via Dodecaneso 35, 16146 Genova, ITALY

³ Istituto Nazionale per la Ricerca sul Cancro, Largo R. Benzi 10, 16132 Genova, ITALY

Abstract. Multimodal medical imaging (MMI) volumes can be derived by spatial correlating intensity distributions from a number of different diagnostic volumes with complementary information. An unsupervised approach to MMI volumes segmentation is recommended by many authors. Due to complexity of the data structure, this kind of segmentation is a very challenging task, whose main step is clustering in a multidimensional feature space. The partial volume effect originated by the relatively low resolution of sensors produces borders not strictly defined between tissues. Therefore memberships of voxels in boundary regions are intrinsically fuzzy and computer assisted unsupervised fuzzy clustering methods turn out to be particularly suited to handle the segmentation problem. In this paper a number of clustering methods (HCM, FCM, MEP-FC, PNFCM) have been applied to this task and results have been compared.

Keywords. Multimodal medical volumes, segmentation, fuzzy clustering, neuro-fuzzy possibilistic c-means

1 Introduction

Nowadays, medical images are obtained by many different acquisition modalities, including X-ray tomography (CT), magnetic resonance imaging (MRI), single photon emission tomography (SPECT), positron emission tomography (PET), ultrasounds (US), etc. [10].

Multimodal volumes can be derived from a set of such different diagnostic volumes carrying complementary information (e.g., both structural and functional) provided by medical imaging technology, for fully correlating information about the same patient. The visual inspection of a large set of such volumetric images permits only partially to the physician to exploit the whole global information.

Therefore, computer-assisted approaches may be helpful in the clinical oncological environment as support to diagnosis in order to delineate volumes to be treated by radiotherapy and surgery, and to assess quantitatively (in terms of tumor mass or detection of metastases) the effect of oncological treatments.

The extraction of such volumes or other entities of interest from imaging data is named *segmentation* and is usually performed, in the image space, by defining sets of voxels with similar features within a whole multimodal volume.

In this paper we present and discuss some clustering algorithms that have been proposed in the fuzzy set literature, and we apply them to the segmentation of multimodal medical images (MMIs). In particular we consider the Fuzzy C-Means (FCM) [2], the Maximum Entropy Principle based Fuzzy Clustering (MEP-FC) [14], the Possibilistic C-Means (PCM) [7], and a new algorithm named Possibilistic Neuro-Fuzzy C-Means (PNFCM).

In the next Section we will discuss the application of the fuzzy clustering to the segmentation of MMI volumes. In Sections 3,4,5,6 we will present the FCM, MEP-FC, PCM and PNFCM algorithms. In Sections 7 we will present the data set whereas in Section 8 we will discuss our results. Conclusions are reported in Section 9.

2 Fuzzy Approach to Segmentation of Multimodal Medical Volumes

The segmentation of MMI volumes can be described as the definition of clusters, in the multimodal feature space, whose points are associated to similar sets of intensity values in the different images. Let us consider a multimodal volume resulting from the spatial registration of a set of s different imaging volumes. We may notice that its voxels are associated with an array of s values, each representing the intensity of a single feature in a voxel. In other words, the s different intensity values related to all the voxels in such multimodal volumes can be viewed as the coordinates of the voxels within an s -dimensional feature space where multimodal clustering can be performed.

Two different spaces have therefore to be considered for a more complete description of the segmentation problem: an image space (usually 3D) defined by the spatial coordinates of the data set, and a multidimensional feature space, as described before. The interplay between these two spaces results very important in the task of understanding the data structure. As a consequence, an efficient segmentation of multimodal medical imaging volumes is an inherently complex task in which each component of the data structure, that is, the spatial distribution of the values of a single feature, must be considered together with all the other components. Such a task may be helpful in the clinical oncological environment to delineate volumes to be treated by radiotherapy and surgery and to assess quantitatively (in terms of tumor mass or detection of metastases) the effect of oncological treatments.

Due to severe drawbacks of supervised segmentation methods, when applied in clinical practice, an unsupervised approach has been followed in many recent papers [3,11,12,15,16]. Unsupervised approaches self-organize the implicit structure of data and make clustering of the feature space independent of the user's definition of training regions [1] and, finally, the multidimensionality of data is definitely better exploited.

It is worth noting that unsupervised methods have been shown to be more robust to noise in discrimination of different tissues than techniques based on edge detection due to the high noise level, or supervised approaches [3].

In a previous paper [15], we presented an interactive segmentation system whose core was an unsupervised neural network, named Capture Effect Neural Network (CENN) [6] (Appendix A). In order to overcome its limits in applications with high dimensionality features spaces and a non-negligible variability of its results for classes poorly represented in the data distribution, we have studied potential benefits of applying fuzzy clustering methods to the segmentation of multimodal medical images.

Fuzzy clustering methods are potentially very useful in our case due to some intrinsic characteristics of the problem of MMI volumes segmentation. In fact, in medical images, uncertainty is largely embedded in data, due, besides the noise in acquisition, to partial volume effects. This means that voxel values, especially at the borders between volumes of interest, correspond to mixtures of different anatomical tissues, because of the low resolution of sensors. As a consequence, borders between tissues are not strictly defined and memberships in boundary regions are intrinsically fuzzy. Moreover the addition of some kind of smoothness to the voxel classification, through fuzzy clustering methods, may be very helpful in order to better define surfaces of the anatomical objects described by segmentation.

3 The Fuzzy C-Means Algorithm

The first algorithm we introduce was proposed by Bezdek [2] as an improvement of the classic Hard C-Means clustering algorithm [4].

Let us assume as a fuzzy C-Means Functional

$$J_m(U, Y) = \sum_{k=1}^n \sum_{j=1}^c (u_{jk})^m E_j(x_k) \quad (1)$$

where

$\Omega = \{x_k | k \in [1, n]\}$ is a training set containing n unlabeled samples;

$Y = \{y_j | j \in [1, c]\}$ is the set of centers of clusters;

$E_j(x_k)$ is a dissimilarity measure (distance or cost) between the sample x_k and the center y_j of a specific cluster j ;

$U = [u_{jk}]$ is the $c \times n$ fuzzy c-partition matrix, containing the membership values of all samples in all clusters;

$m \in (1, \infty)$ is a control parameter of fuzziness.

The clustering problem can be defined as the minimization of J_m with respect to Y , under the *probabilistic constraint*:

$$\sum_{j=1}^c u_{jk} = 1 \quad (2)$$

The Fuzzy C-Means (FCM) algorithm proposed by Bezdek [2] consists in the iteration of the following formulas:

$$y_j = \frac{\sum_{k=1}^n (u_{jk})^m x_k}{\sum_{k=1}^n (u_{jk})^m} \quad \text{for all } j \quad (3)$$

and

$$u_{jk} = \begin{cases} \left(\frac{E_j(x_k)}{\sum_{l=1}^c E_l(x_k)} \right)^{\frac{2}{m-1}} & \text{if } E_j(x_k) > 0 \quad \forall j, k \\ 1 & \text{if } E_j(x_k) = 0 \quad \text{and } u_{ik} = 0 \quad \forall i \neq j \end{cases} \quad (4)$$

where, in the case of the Euclidean space:

$$E_j(x_k) = \|x_k - y_j\|^2 \quad (5)$$

It is worth noting that if one chooses $m = 1$ the fuzzy C-Means Functional J_m (Eq. 1) reduces to the expectation of the global error (which we denote as $\langle E \rangle$):

$$\langle E \rangle = \sum_{k=1}^n \sum_{j=1}^c u_{jk} E_j(x_k) \quad (6)$$

and the FCM algorithm becomes the classic Hard C-Means algorithm [4].

4 The MEP-FC Algorithm

The Maximum Entropy Principle proposed by Jaynes in the fifties [9] has been recently applied to fuzzy clustering by Rose, Gurewitz and Fox [13,14].

Let p_{jk} be the probability distribution of k -th pattern of the training set Ω to j -th cluster and

$$H(p_{11}, p_{12}, \dots, p_{cn}) = -K \sum_{j=1}^c \sum_{k=1}^n p_{jk} \ln p_{jk} \quad (7)$$

the Shannon entropy [17] of Ω .

By maximizing H under the constraints of Eqs. (6) and (2), the resulting membership functions of samples in clusters are Gibbs distributions [9]:

$$u_{jk} = \frac{e^{-\beta E_j(x_k)}}{Z_k} \quad (8)$$

where

$$Z_k = \sum_{l=1}^c e^{-\beta E_l(x_k)} \quad (9)$$

is a normalization factor named Partition Function. From a Statistical Mechanics point of view, the Lagrange multiplier β is interpreted as the inverse of temperature T ($\beta = 1/T$). Moreover, it can be interpreted as a control parameter of fuzziness. When β increases, the associations of samples with clusters become crisper.

The limit cases are:

for $\beta \rightarrow 0^+$ we have $u_{jk} = 1/c$ for all j, k , i.e., each sample is equally associated with each cluster;

for $\beta \rightarrow +\infty$ we have $u_{jk} = 1$ if the sample belongs to the cluster j , and $u_{ik} = 0$ for all $i \neq j$, $i \in [1, c]$, i.e., each sample is associated with only one cluster (hard limit).

Let us define the Effective Error (also named the Free Energy, by analogy to Statistical Mechanics)

$$F \equiv -\frac{1}{\beta} \ln Z \quad (10)$$

where $Z = \prod_k Z_k$ is named the Total Partition Function.

One can demonstrate that

$$F = -\frac{1}{\beta} H_{\max} + \langle E \rangle \quad (11)$$

and then

$$\lim_{\beta \rightarrow \infty} F = \langle E \rangle \quad (12)$$

This limit allows us to find the solution of the constrained minimization of $\langle E \rangle$ by performing a so-called *Deterministic Annealing* on F , as proposed by Rose, Gurewitz and Fox [13,14]. This method, which we name Maximum Entropy Principle based Fuzzy Clustering (MEP-FC) method, starts by minimizing F at a

high T , for which there is a unique solution $u_{jk} = 1/c$ for all j, k , and then reduces T , until the hard limit is reached.

In the algorithm used here, we assume, as proposed in [13,14], $E_j(x_k) = \|x_k - y_j\|^2$ and for each value of β we perform a minimization of F with respect to Y by iterating the following formula:

$$y_j = \frac{\sum_{k=1}^n u_{jk} x_k}{\sum_{k=1}^n u_{jk}} \quad (13)$$

It is worth noting that, whereas standard clustering algorithms (included the FCM one) need to specify the number of clusters, the MEP-FC algorithm can start with an over-dimensioned number of clusters. At high temperatures, all centers collapse at a unique point, and then, during annealing, "natural" clusters differentiate.

5 The Possibilistic C-Means Algorithm

In the possibilistic approach to clustering proposed by Keller and Krishnapuram [7,8], the membership function or the degree of *typicality* of a point in a *fuzzy* set (or cluster) is assumed to be absolute. In other words, the degree of typicality does not depend on the membership values of the same point in other clusters contained in the problem domain.

By contrast, many clustering approaches impose a probabilistic constraint, according to which the sum of the membership values of a point in all the clusters must be equal to one. As a consequence, HCM [4], FCM [2], MEP-FC [13], and many other clustering methods assuming the probabilistic constraint cannot generate membership functions whose values can be interpreted as degrees of *typicality*.

In [7,8], Krishnapuram and Keller presented two versions of a Possibilistic C-Means (PCM) algorithm that avoids the assumption of the probabilistic constraint.

The PCM is based on the relaxation of the probabilistic constraint in order to interpret in a *possibilistic* sense the membership function or degree of *typicality*.

Let $\Omega = \{x_k | k \in [1, n]\}$ be the set of unlabeled samples; $Y = \{y_j | j \in [1, c]\}$ be the set of cluster centers (or prototypes); and $U = [u_{jk}]$ be the *fuzzy membership matrix*.

In the PCM, the elements of U fulfil the following conditions:

$$u_{jk} \in [0, 1] \quad \forall j, k \quad (14)$$

$$0 < \sum_{k=1}^n u_{jk} < n \quad \forall j \quad (15)$$

$$\forall_j u_{jk} > 0 \quad \forall k \quad (16)$$

The first Possibilistic C-Means algorithm (PCM-I) proposed by Krishnapuram and Keller [7] is based on a modification of the objective function of FCM [2]. In this case, one must supply the values of some parameters such as the *fuzzifier parameter*, and others regulating the weight of the spread of membership functions [7].

In [8], Krishnapuram and Keller proposed a new formulation of Possibilistic C-Means (PCM-II) based on modification the cost function of the HCM [4] (instead of the FCM) in order to avoid, in this way, the determination of the fuzzifier parameter.

The objective function of the PCM-II contains two terms, the first one is the objective function of the HCM [4], while the second is a regularizing term, forcing the values u_{jk} to be greatest as possible, in order that points with a high degree of typicality with respect to a cluster may have high u_{jk} values, and points not very representative may have low u_{jk} values in all clusters:

$$J(U, Y) = \sum_{k=1}^n \sum_{j=1}^c u_{jk} E_j(x_k) + \sum_{j=1}^c \rho_j \sum_{k=1}^n (u_{jk} \ln u_{jk} - u_{jk}) \quad (17)$$

where $E_j(x_k) = \|x_k - y_j\|^2$ is the square of the Euclidean distance, and the parameter ρ_j depends on the distribution of point in the j -th cluster.

It is worth noting that if the second term of $J(U, Y)$ is omitted, the elimination of the probabilistic constraint leads to a trivial solution of the minimization of the remaining cost function, that is $u_{jk} \in [0, 1] \quad \forall j, k$.

If one searches for clusters with similar distribution, ρ_j could be set to the same value for each cluster. In general, it is assumed that ρ_j depends on the average size and on the shape of the j -th cluster.

As demonstrated by Krishnapuram and Keller [8], the couple (U, Y) minimizes J under the constraints (14), (15) and (16) only if:

$$y_j = \frac{\sum_{k=1}^n u_{jk} x_k}{\sum_{k=1}^n u_{jk}} \quad \forall j \quad (18)$$

and

$$u_{jk} = \exp\left\{-\frac{E_j(x_k)}{\rho_j}\right\} \quad \forall j, k \quad (19)$$

This theorem provides the conditions needed in order to minimize the cost function $J(U, Y)$. Eq.s (18) and (19) can be interpreted as formulas for recalculating the membership functions and the cluster centers.

A bootstrap clustering algorithm is anyway needed before starting PCM in order to obtain an initial distribution of prototypes in the feature space and to estimate some parameters used in the algorithm.

By considering an FCM bootstrap for the PCM, the following definition of ρ_j is initially used [7,8]:

$$\rho_j \equiv K \frac{\sum_{k=1}^n (u_{jk})^m E_j(x_k)}{\sum_{k=1}^n (u_{jk})^m} \quad (20)$$

where $m \in (1, +\infty)$ is the *fuzzifier* parameter used by the FCM, and K is a proportional parameter. This definition makes ρ_j proportional to the mean value of the *intracluster distance*, and critically depends on the choice of K (in [7] it has been suggested $K = 1$).

In a following optional refinement step a second definition of ρ_j is used:

$$\rho_j = \frac{\sum_{x_k \in (\pi_j)_\alpha} E_j(x_k)}{|(\pi_j)_\alpha|} \quad (21)$$

where $(\pi_j)_\alpha$ is the set of points of the j -th cluster whose membership function is above a given threshold α (α -cut).

This second definition makes ρ_j as a more robust estimator of the mean value of the *intracluster distance* calculated by using points belonging to the α -cut.

The PCM starts from the solutions of the bootstrap clustering algorithm and is based on two Lloyd-Picard iterations, the first one using Eq. (20), and the second using Eq. (21) [7].

The use of FCM as a bootstrap for the PCM, involves the problem of the estimation of the K parameter, the fuzzifier parameter m and of the number of clusters c . However, sometimes, even if c has been over-dimensioned in FCM, the following PCM step aggregates close clusters from FCM, characterized by large distributions of points, in one unique cluster, thus giving rise to a bias if the FCM is used as a bootstrap for the PCM. We suggest this is due to the fact that *intracluster distances*

from an algorithm with a probabilistic constraint are used to calculate membership values for a possibilistic algorithm and this may produce a misdefinition of the ρ_j 's.

For these reasons we studied a bootstrap for the PCM based on the Capture Effect Neural Network (CENN) [5] that can find automatically a robust estimation of the number of *natural* clusters, and of their centers and radii (see Appendix). In particular the estimation of radii is a very helpful information that is strictly related with the *intracluster distance* [12].

Possibilistic Neuro-Fuzzy C-Means (PNFCM) Algorithm

CENN Bootstrap

- *train and label the Capture Effect Neural Network;*
- *obtain c , ρ_j , and y_j^0 ;*
- *compute $U^{(0)}$ using Eq. (19);*
- *set the iteration counter to $l=0$ and the stop parameter ε .*

PCM-II Basic Iteration

Repeat

- *update the prototypes $y_j^{(l+1)}$ using Eq. (18);*
- *compute $U^{(l+1)}$ using Eq. (19);*
- *increment l ;*

Until

$$\forall_j \|y_j^{(l+1)} - y_j^l\| \leq \varepsilon;$$

Merging redundant clusters

- *group clusters with distance less than 10ε .*

Fig. 1. Description of the PNFCM algorithm

In the following Section we describe the application of CENN as a bootstrap for the PCM in order to obtain a newly defined Possibilistic Neuro-Fuzzy C-Means algorithm (PNFCM).

6 The Possibilistic Neuro-Fuzzy C-Means Algorithm

In our use of CENN as an unsupervised clustering algorithm for the segmentation problem of multimodal medical images [15] we found some limits of this neural network in problems with high dimensionality. On the contrary, especially when the feature space has few dimensions, CENN shows the capability of obtain automatically a robust estimation of the number of *natural* clusters c , and of their

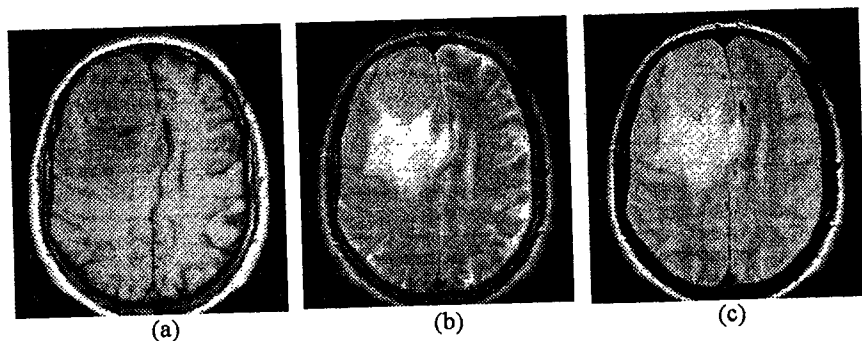


Fig. 2. T1 (a), T2 (b) and PD (c) MRI images with meningioma

centers y_j and radii r_j , that are related with ρ_j (i.e., $\rho_j = f(r_j)$). This makes CENN a robust and un-biased bootstrap procedure to be used in conjunction with the PCM, overcoming the defects of FCM, pointed out in the previous Section.

The description of the application of CENN as a bootstrap algorithm for PCM-II is presented in Fig. 1.

It is worth pointing out that in the PNFCM algorithm the number of clusters c is not a constraint, but is automatically found in three main steps: the CENN Bootstrap step is initialized with a very high-dimensional value of c and obtains a first evaluation of the number of natural clusters, the following PCM-II Basic Iteration draws redundant cluster centers and the last Merging Rule step unifies clusters with close centers.

7 Data Set and Feature Space

The data set (Fig. 2.) consists of a multimodal transverse slice of the head composed by three different (T1-weighted, T2-weighted, Proton Density) MRI images of the head of an individual with meningioma. The images are 256×256 with 255 gray levels. The tumor is located in the right frontal lobe and appears bright on the T2-weighted image and dark on the T1-weighted image. A large amount of edema is surrounding the tumor and appears very bright on the T2-weighted image. The fusion of the data sets produced a three-variate volume.

Each triplet of voxel intensity in the volume was represented by a point in a 3D feature space, whose coordinates represented the intensity values in that voxel of each volume belonging to the multivariate volume. In Fig. 2 the three-dimensional feature space resulting from this data set is shown. It is worth noting that the usefulness of segmentation in medical imaging is related to the balance of two conflicting actions performed during the processing sequence, namely, the elimination of noise and redundancy from original images and the preservation of significant information in the segmented image.

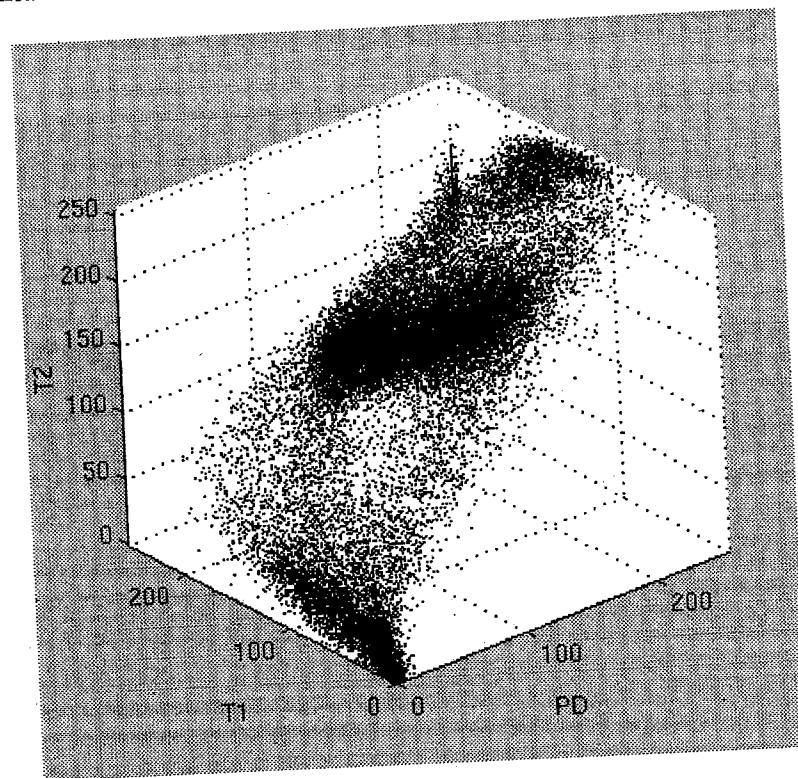


Fig. 3. Three-dimensional feature space

8 Results and Discussion

Starting from previous considerations, let us compare the results produced by the different clustering algorithms. In order to obtain a more quantitative comparison between results from the different algorithms, we made an indirect comparison of the image segmented by each algorithm, with a segmented image accepted by a pool of skilled clinicians, considered as a reference image.

A quantitative evaluation of the similarity (σ_{testj}) of the result of a segmentation algorithm with the reference segmentation is given by:

$$\sigma_{testj} \equiv \frac{A_{testj} \cap A_{refj}}{A_{testj} \cup A_{refj}} \quad (22)$$

where A_{testj} is the area of the j -th class calculated in some test situation and A_{refj} is the area of the same j -th class calculated in a reference situation. The similarity evaluation for each algorithm and for each class are shown in Table 1.

The number of classes has been imposed to 8 (eight) for the HCM and the FCM algorithms as it results from the accepted supervised segmentation. The MEP-FC

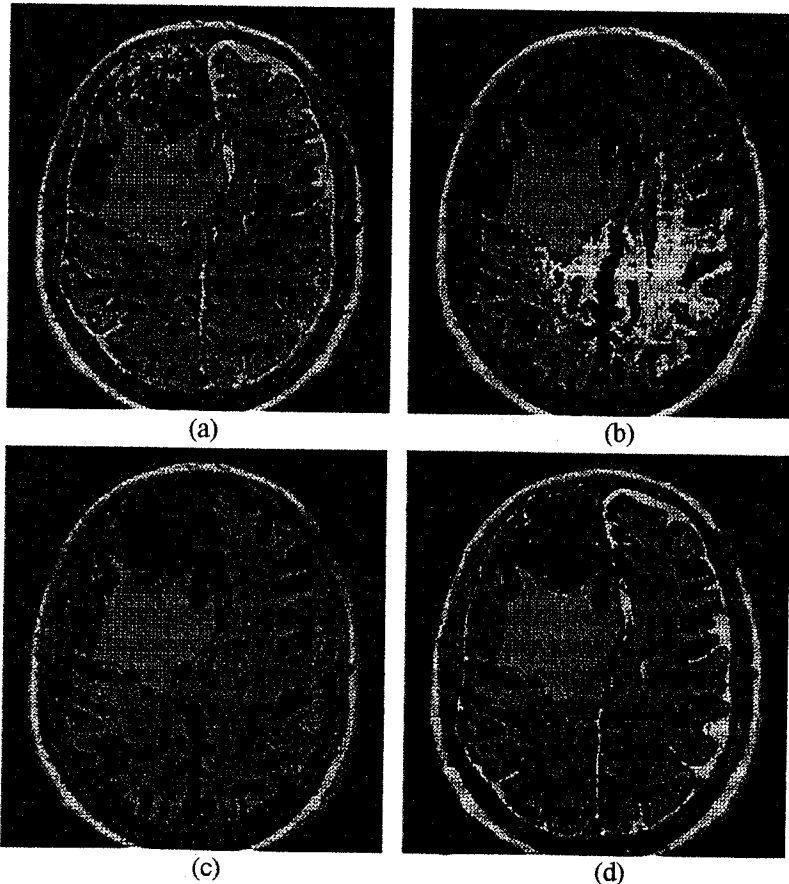


Fig. 4. Segmentation images by HCM (a), FCM (b), MEP-FC (c) and PNFCM (d) algorithms

Table 1. Similarity evaluations of results by HCM, FCM, MEP-FC and PNFCM with a supervised reference segmentation performed by skilled experts. Each value is the average of three independent runs of clustering algorithms

σ_{testj}	HCM	FCM	MEP-FC	PNFCM
Tumor	.09	.59	.44	.74
Edema	.76	.79	.79	.95
Gray matter	.53	.69	.68	.76
White matter	.77	.50	.83	.94

and the PNFCM algorithms have been supposed to autonomously find the right number of classes.

Besides quantitative results shown in Table 1 some more clinical considerations may be helpful in evaluating the different algorithms. With the HCM algorithm (Fig. 4a) we may notice that edema is correctly evidenced but tumor and gray matter result as an unique class. Moreover white matter results overestimated. If the FCM segmentation is performed, results (Fig. 4b) show that tumor is separated from edema but the separation between tumor and gray matter is partially lost. Moreover white matter is very noisy defined and results confused with skull. The MEP-FC algorithm (Fig. 4c) not always finds the right number of classes and produces an unsatisfactory separation between tumor and gray matter.

As regards the PNFCM algorithm, the application of the CENN neural network to the data set gives as a result the number c of centroids, their coordinates y_j and their radii r_j . In our experiments we found a good evaluation of ρ_j as $\rho_j = \sqrt[D]{r_j}$ where D is the dimensionality of the feature space. After the neural bootstrap with CENN, the PCM-II step was performed, using $\varepsilon = 0.01$ as stop parameter and then the merging method was applied in order to find the final cluster centers. The CENN algorithm has autonomously found ten classes with some redundancy. By applying the PCM-II algorithm to the results of CENN, better results with only eight classes have been obtained (Fig. 4d) that improve the segmentation of tumor and edema, while retaining the good performances about gray matter and skull.

In general we may say that the PCM-II algorithm in sequence to CENN (PNFCM) is able to keep separate in the feature space classes with higher probability density and therefore with greater degree of typicality and in the meantime to merge noisy classes in order to obtain a better homogeneity.

We must notice that the convergence times of our fuzzy clustering algorithms when applied to real multimodal medical volumes result too long to be accepted in the clinical practice, due to the huge amount of data. Therefore, we studied possible solutions able to reduce the data set in order to speed up calculation. With this aim we randomly sampled the training set Ω , but instead of using the same Reduced Data Base (RDB) for the whole algorithm, we randomly resampled a new

RDB for each training epoch. In Fig. 5 a quantitative comparison is presented of gray matter segmentation results obtained by HCM, FCM, MEP-FC, and PNFCM algorithms, with different subsampling percentages, when applied to slice 80 of a healthy patient. The best results are obtained using the PNFCM for which σ_{refj} is above 95% until sampling of 20%, and above 90% until sampling of 10%.

9 Conclusions

In this paper we have presented some fuzzy clustering algorithms, including HCM, FCM, MEP-FC, PNFCM, and we have compared them in the application to multimodal medical volumes segmentation.

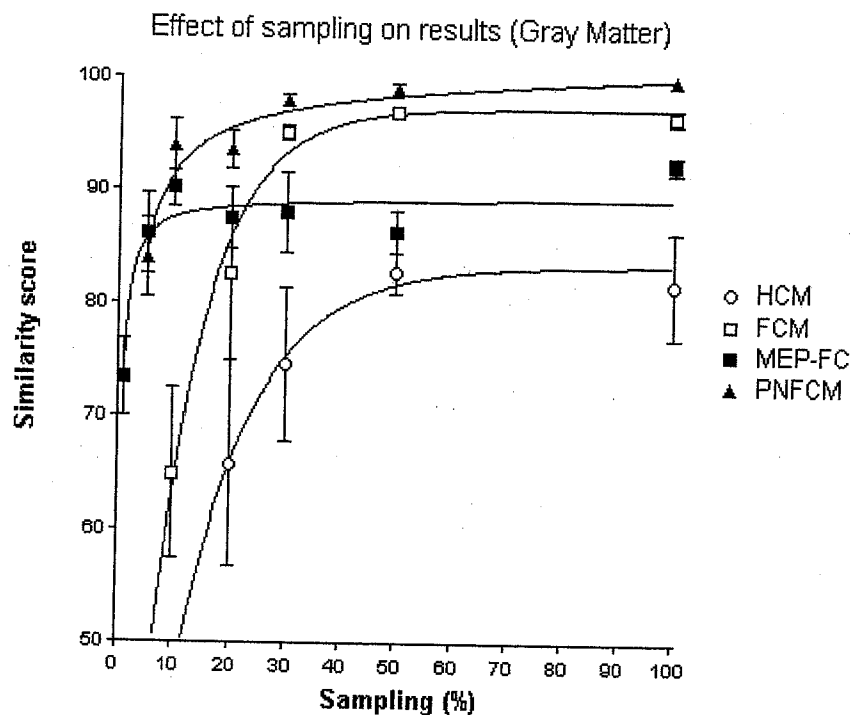


Fig.5. Quantitative comparison of clustering algorithms with different subsampling percentages. Each similarity value (%) is the average of three independent runs of clustering algorithms

The higher performances in the MMI segmentation task obtained by the PNFCM algorithm with respect to the other clustering techniques studied can be related to the consistency of the PCM's theoretical basis with the specific features of medical images. In fact, *membership values (degrees of typicality) of voxels in a particular*

anatomical tissue (cluster) are characteristic of the tissue and they should not depend on voxel membership values in other tissues.

Acknowledgements

This work was partially funded by MURST and INFN Progetto Sud TELEMA.

Appendix A: The Capture Effect Neural Network

The Capture Effect Neural Network (CENN) is a self-organizing neural network able to take into account the local characteristic of the point-distribution (*adaptive resolution clustering*). CENN combines standard competitive self-organization of the weight-vectors with a non-linear mechanism of adaptive local modulation of receptive fields (RF) of neurons (*Capture Effect*). The learning of CENN is composed by two steps:

- *Training step* where an abundant number of prototypes is used (defined by their weight vectors and RF dimension) for vector quantization of data;
- *Clustering step* where prototypes are grouped in order to represent the cluster distributions.

After learning:

- The distribution of the prototypes in the feature space approaches the optimal vector quantization scheme of the distribution of input data, i.e. approximates the mixture probability density function;
- The radial size of the RF of each neuron reaches a stable value which is strongly related to the spatial density of input data locally around the center of the RF itself, that is the weight-vector of the neuron.

It is worth noting that the clustering step of CENN gives automatically a robust estimation of the number c of centroids and of their coordinates y_j and radii r_j .

Moreover we can assume that $\rho_j = f(r_j)$. As a consequence it seems useful to use the CENN instead of the FCM as a bootstrap for the PCM.

References

1. A.M. Bensaid, L.O. Hall, L.P. Clarke, and R.P. Velthuizen (1991): MRI segmentation using supervised and unsupervised methods. In: *Proc. 13th IEEE Eng. Med. Biol. Conf.*, Orlando. IEEE, pp.483-489.
2. J.C. Bezdek (1981): *Pattern Recognition with Fuzzy Objective Function Algorithms*, Plenum Press, New York.
3. J.C. Bezdek, L.O. Hall, and L.P. Clarke. Review of MR image segmentation techniques using pattern recognition, *Med. Phys.*, **20**(1993), pp.1033-1048.
4. R.O. Duda and P.E. Hart (1973): *Pattern Classification and Scene Analysis*, Wiley, New York.

RDB for each training epoch. In Fig. 5 a quantitative comparison is presented of gray matter segmentation results obtained by HCM, FCM, MEP-FC, and PNFCM algorithms, with different subsampling percentages, when applied to slice 80 of a healthy patient. The best results are obtained using the PNFCM for which σ_{ref} is above 95% until sampling of 20%, and above 90% until sampling of 10%.

9 Conclusions

In this paper we have presented some fuzzy clustering algorithms, including HCM, FCM, MEP-FC, PNFCM, and we have compared them in the application to multimodal medical volumes segmentation.

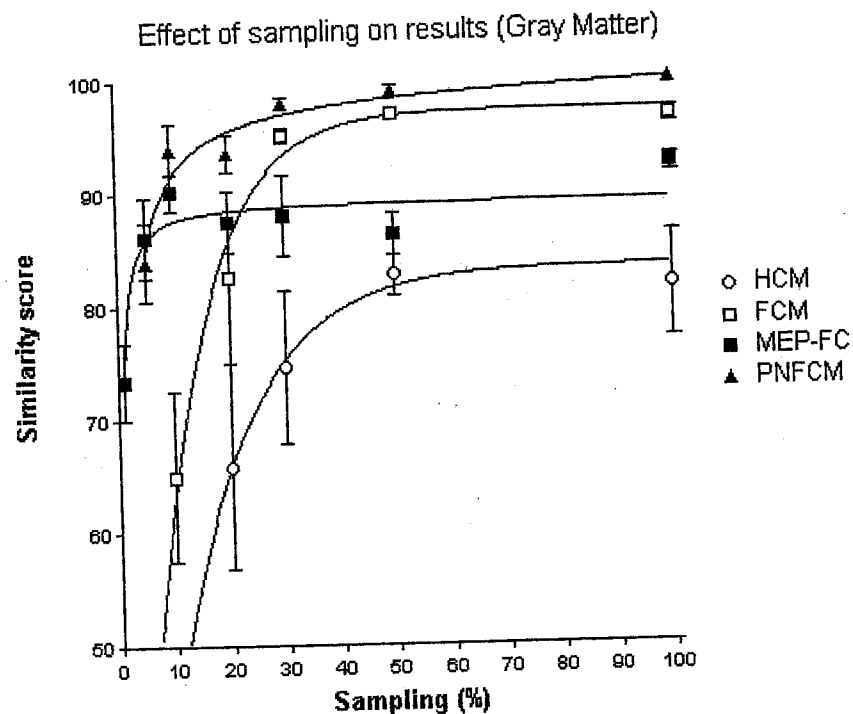


Fig. 5. Quantitative comparison of clustering algorithms with different subsampling percentages. Each similarity value (%) is the average of three independent runs of clustering algorithms

The higher performances in the MMI segmentation task obtained by the PNFCM algorithm with respect to the other clustering techniques studied can be related to the consistency of the PCM's theoretical basis with the specific features of medical images. In fact, *membership values (degrees of typicality) of voxels in a particular*

anatomical tissue (cluster) are characteristic of the tissue and they should not depend on voxel membership values in other tissues.

Acknowledgements

This work was partially funded by MURST and INFN Progetto Sud TELEMA.

Appendix A: The Capture Effect Neural Network

The Capture Effect Neural Network (CENN) is a self-organizing neural network able to take into account the local characteristic of the point-distribution (*adaptive resolution clustering*). CENN combines standard competitive self-organization of the weight-vectors with a non-linear mechanism of adaptive local modulation of receptive fields (RF) of neurons (*Capture Effect*). The learning of CENN is composed by two steps:

- *Training step* where an abundant number of prototypes is used (defined by their weight vectors and RF dimension) for vector quantization of data;
- *Clustering step* where prototypes are grouped in order to represent the cluster distributions.

After learning:

- The distribution of the prototypes in the feature space approaches the optimal vector quantization scheme of the distribution of input data, i.e. approximates the mixture probability density function;
- The radial size of the RF of each neuron reaches a stable value which is strongly related to the spatial density of input data locally around the center of the RF itself, that is the weight-vector of the neuron.

It is worth noting that the clustering step of CENN gives automatically a robust estimation of the number c of centroids and of their coordinates y_j and radii r_j .

Moreover we can assume that $\rho_j = f(r_j)$. As a consequence it seems useful to use the CENN instead of the FCM as a bootstrap for the PCM.

References

1. A.M. Bensaid, L.O. Hall, L.P. Clarke, and R.P. Velthuizen (1991): MR segmentation using supervised and unsupervised methods. In: *Proc. 13th IEEE Eng. Med. Biol. Conf.*, Orlando. IEEE, pp.483-489.
2. J.C. Bezdek (1981): *Pattern Recognition with Fuzzy Objective Function Algorithms*, Plenum Press, New York.
3. J.C. Bezdek, L.O. Hall, and L.P. Clarke. Review of MR image segmentation techniques using pattern recognition, *Med. Phys.*, 20(1993), pp.1033-1048.
4. R.O. Duda and P.E. Hart (1973): *Pattern Classification and Scene Analysis* Wiley, New York.

5. F. Firenze and P. Morasso (1993): The capture effect model: a new approach to self-organized clustering. In: *Sixth International Conference. Neural Networks and their Industrial and Cognitive Applications. NEURO-NIMES 93. Conference Proceedings and Exhibition Catalog*, Nimes, France. pp. 65-54.
6. F. Firenze, A. Schenone, F. Acquarone, M. Gambaro, F. Masulli (1995): An "adaptive resolution" analysis of multivariate medical images via unsupervised neural network based clustering. *Proc. EUFIT 95*, Aachen, , pp. 1690-1694.
7. R. Krishnapuram and J.M. Keller (1993): A possibilistic approach to clustering. *IEEE Transactions on Fuzzy Systems*, 1: pp.98-110.
8. R. Krishnapuram and J.M. Keller (1996): The Possibilistic C-Means Algorithm: insights and recommendations, *IEEE Transactions on Fuzzy Systems*, 4: pp.385-393.
9. E.T. Jaynes (1957): Information theory and statistical mechanics, *Physical Review* 106, pp. 620-630.
10. M.N. Maisey et al. (1992): Synergistic Imaging, *Eur. J. Nucl. Med.*, 19, pp.1002-1005.
11. F. Masulli, P. Bogus, A. Schenone, and M. Artuso (1997): Fuzzy clustering methods for the segmentation of multivariate images. In M. Mares, R. Mesia, V. Novak, J. Ramik, and A. Stupnanova, (editors), *Proceedings of the 7th International Fuzzy Systems Association World Congress IFSA'97*, volume III, Prague, Academia, pp. 123-128.
12. F. Masulli, and A. Schenone. A fuzzy clustering based segmentation system as support to diagnosis in medical imaging. *Artificial Intelligence in Medicine*, 1998 (in press).
13. K. Rose, E. Gurewitz, and G. Fox (1993): A deterministic annealing approach to clustering, *Pattern Recognition Letters*, 11:589-594, 1990.
14. K. Rose, E. Gurewitz, and G. Fox. Constrained clustering as an optimization method, *IEEE Transactions on Pattern Analysis and Machine Intelligence*, 15:pp.785-794.
15. Schenone, F. Firenze, F. Acquarone, M. Gambaro, F. Masulli, and L. Andreucci (1996): Segmentation of multivariate medical images via unsupervised clustering with adaptive resolution. *Computerized Medical Imaging and Graphics*, 20:pp.119-129.
16. Schenone, F. Masulli, and M. Artuso. A neural bootstrap for the Possibilistic C-Means Algorithm. In: F.C. Morabito, (editor), *Advances in Intelligent Systems*, pp. 359-366, Amsterdam, 1997. IOS Press.
17. C.E. Shannon, and W. Weaver (1949): *The mathematical theory of communication*, University of Illinois Press, Urbana.

Fuzzy Clustering for Parametric Map Construction in Myocardial Perfusion Magnetic Resonance Images

Faiza Belhoul, Abdel-Ouahab Boudraa,
Marc Janier and Pierre Croisille

CREATIS, CNRS UMR 5515 Affiliated to INSERM
INSA-502
69621 Villeurbanne
France

E-mail: behloul@creatis.insa-lyon.fr

Abstract. Ischemic heart disease is due to an imbalance of blood flow demand and supply. In clinical settings, nuclear imaging modalities, Single Photon Emission Computed Tomography (SPECT) or Positron Emission Tomography (PET), are used to detect blood flow (perfusion) defects in the myocardium. However, Magnetic Resonance Imaging (MRI) presents the advantage of a better spatial resolution than nuclear methods and a sufficient temporal resolution to detect small perfusion defects that may not be detected by PET or SPECT. Since perfusion analysis can only be derived from time intensity diagrams over a series of images, computer-assisted image evaluation is required. A parametric map that summarizes the temporal behavior of the pixels within the heart image is necessary. In nuclear medicine, the parametric map construction is based on a model of the contrast agent used to image the myocardial perfusion over time. In MRI, the definition of such a model is still a challenging issue. This work shows that an unsupervised fuzzy clustering technique may be a good alternative to build a perfusion parametric map. Being unsupervised, this technique does not require a model, and the notions of fuzzy clusters and membership degree are adequate to show the smooth transition between healthy and pathological tissues. However, a careful use of similarity measures for the clustering process is required.

Keywords: Myocardial Perfusion, Magnetic Resonance Imaging, Fuzzy clustering, similarity measures.

1 Introduction

Magnetic Resonance Imaging (MRI) of the heart has gained widespread scientific and clinical acceptance. This noninvasive modality permits acquisition of high resolution images in virtually and tomographic plane useful for